

Paper contributed to the X International Symposium on Lepton and Photon Interactions at High Energies, 23rd-28th July 2001, Rome, Italy.

## Results and plans of the CRESST dark matter search

M. Altmann<sup>b</sup>, G. Angloher<sup>d</sup>, M. Bruckmayer<sup>b</sup>, C. Bucci<sup>a</sup>, S. Cooper<sup>d</sup>,  
 C. Cozzini<sup>b</sup>, P. DiStefano<sup>b</sup>, F. von Feilitzsch<sup>c</sup>, T. Frank<sup>b</sup>, D. Hauff<sup>b</sup>,  
 Th. Jagemann<sup>c</sup>, J. Jochum<sup>c</sup>, R. Keeling<sup>d</sup>, H. Kraus<sup>d</sup>, J. Macallister<sup>d</sup>,  
 F. Pröbst<sup>b,2</sup>, Y. Ramachers<sup>d</sup>, J. Schnagl<sup>c</sup>, W. Seidel<sup>b</sup>, I. Sergeyev<sup>b,1</sup>, M. Stark<sup>c</sup>,  
 L. Stodolsky<sup>b</sup>, H. Wulandari<sup>c</sup>

<sup>a</sup> Laboratori Nazionali del Gran Sasso, I-67010 Assergi, Italy

<sup>b</sup> Max-Planck-Institut für Physik, Föhringer Ring 6, D-80805 Munich, Germany

<sup>c</sup> Technische Universität München, Physik Department, D-85747 Munich, Germany

<sup>d</sup> University of Oxford, Physics Department, Oxford OX1 3RH, U.K.

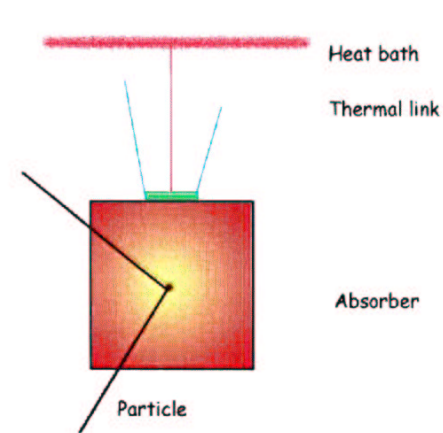
### Abstract

Data taken by CRESST in 2000 with a cryogenic detector system based on 262 g sapphire crystals is used to place limits on WIMP dark matter in the Galactic Halo. The detector is especially sensitive for low-mass WIMPs with spin-dependent cross sections and improves on existing limits in this region. CRESST is now preparing for a second phase, which will use a 10 kg detector consisting of 300 g CaWO<sub>4</sub> crystals with simultaneous detection of phonons and scintillation light to reduce background.

<sup>1</sup> Permanent Address: Joint Institute for Nuclear Research, Dubna, 141980, Russia

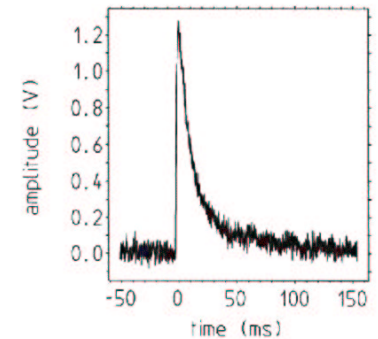
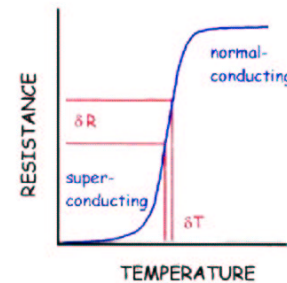
<sup>2</sup>Corresponding author; Tel.: +49 89 32354 270; E-mail: proebst@mppmu.mpg.de

## How Does Phonon Detection Work ?



Phonons created by a particle interaction in the absorber are collected and thermalised by the thermometer

⇒ temperature rise of the thermometer proportional to the deposited energy



Thermometer: superconducting phase transition of W

Operating temperature: ≈ 12 mK

Absorber material: free choice (Al<sub>2</sub>O<sub>3</sub>, Ge, CaWO<sub>4</sub> ...)

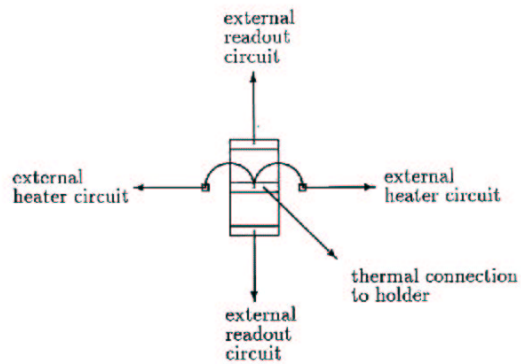


Figure 4: Thermal and electrical connections to thermometer.

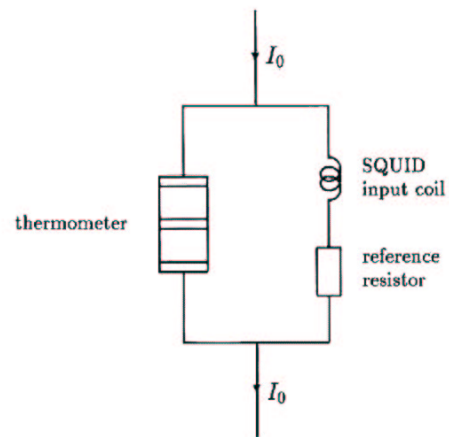
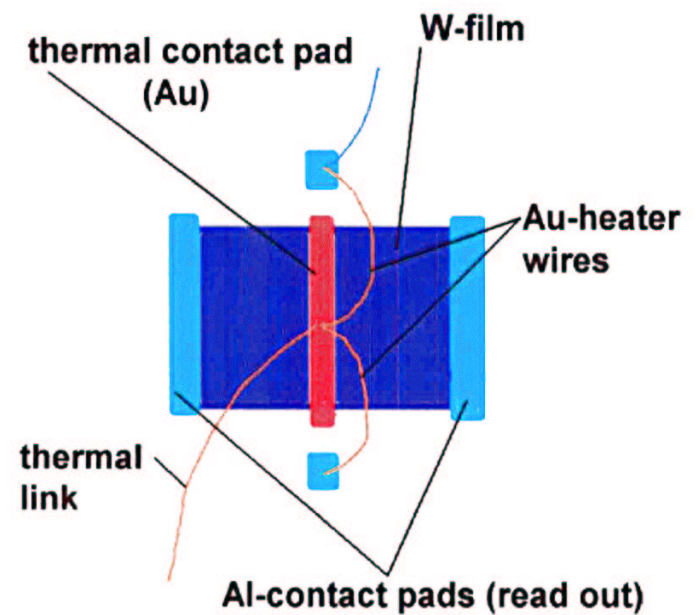


Figure 5: Readout circuit to measure the resistance of the thermometer.

Long Term Stability, Linearisation,  
Energy Calibration,  
Trigger and Cut Efficiency

Heater at the thermometer is used to:

- Apply "DC" - power for temperature control
- Heat pulses to simulate particle pulses



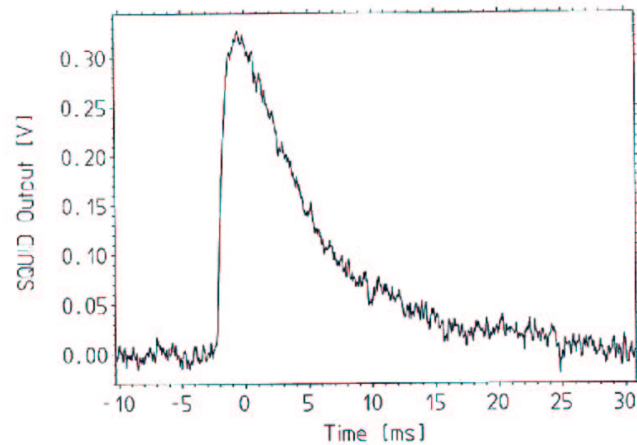
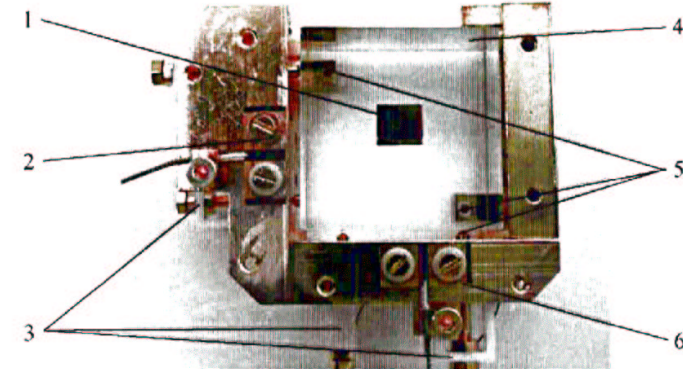


Figure 6: Typical measured pulse of about 6 keV.

a  $\sim 5$  mm long  $25\ \mu\text{m}$  diameter gold wire which was bonded to the gold pad in the center of the W thermometer and two very small Al contact pads on the sapphire crystal to either side of the thermometer. External connections to the two small Al pads were used to apply a controlled voltage across this gold wire. To avoid interaction between the heater circuit and the readout circuit, the place where they connect – the bond spot of the gold wire – was made as small as possible and its long axis was perpendicular to the direction of current flow in the thermometer. The thermometer temperature was kept constant between pulses using the baseline of the SQUID output voltage as the temperature indicator and regulating the voltage to the heater under computer control using a proportional integral algorithm. The heater was additionally used to inject short heat pulses for monitoring the long term stability of the energy calibration and for measuring the trigger efficiency close to threshold.

For the data-acquisition system, the output voltage of the SQUID electronics was split into two branches. One was shaped and ac-coupled to a trigger unit and the other passed through an anti-aliasing filter and was dc-coupled to a 16-bit transient recorder. The time base of the transient recorder was chosen to be  $40\ \mu\text{s}$ , which provided about 20 samples in the rise time of the pulse. The record length of 1024 time bins included a “pre-trigger” region of 256 bins, to record the baseline before the event, and a “post-trigger” region which contained the pulse (Fig. 6). The transient recorder data for each triggered event were written to disk for off-line analysis. After each trigger there was a dead time of  $\sim 25$  ms to allow time for the readout and the next pre-trigger region. Pulses arriving in another detector within half of the post-trigger period of the detector which triggered first were also recorded, including the time delay with respect to the first trigger.

## CRESST Detector



1. W-thermometer
2. Heater contact pads
3. Teflon springs
4. sapphire crystal ( $4*4*4\ \text{cm}^3$ )
5. crystal support tips
6. read-out contact pads

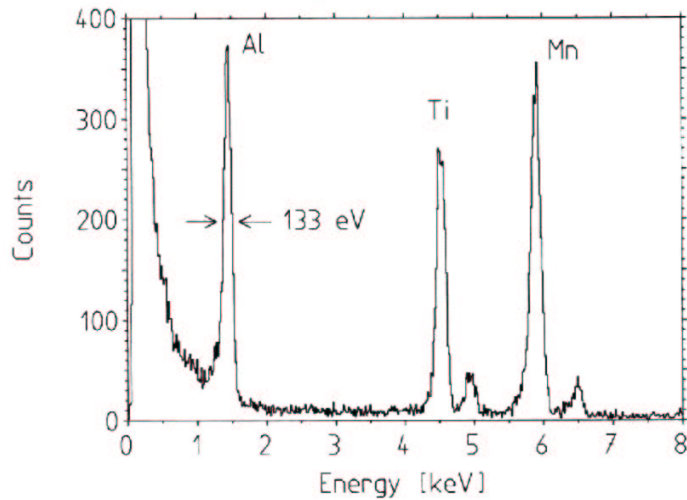


## CRESST I

Detector size:  $4 \times 4 \times 4 \text{ cm}^3$ , 262 g

Operating temperature: 12 mK

262 g sapphire crystal



energy resolution: 133eV @ 1.5 keV

stable and reproducible operation

⇒ excellent performance

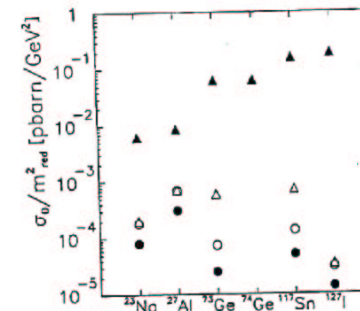
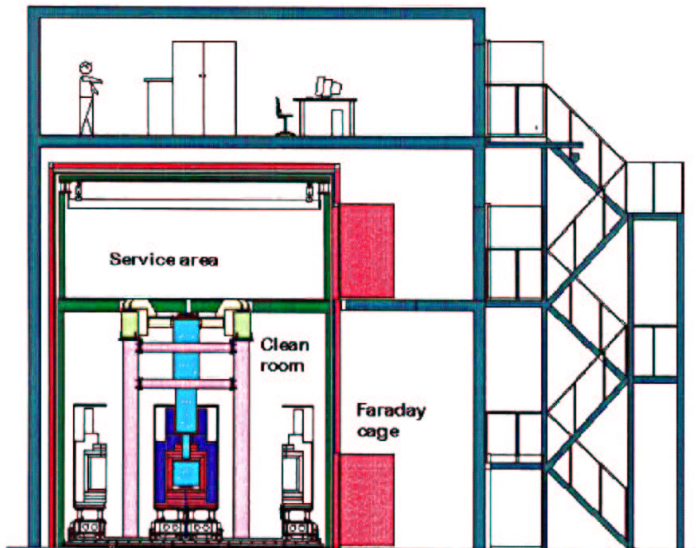


Figure 24: Cross section  $\sigma_0$  (SI+SD) normalized to the reduced mass squared for different materials and neutralino compositions. Solid triangles: zino-higgsino mixture with 40% zino composition. Open triangles: pure higgsino. Solid circles: pure bino. Open circles: pure photino. The cross sections are calculated for set B with  $\tan\beta=2$ ,  $M_A=50$  GeV and  $\alpha = -1.24$ . As can be seen in Fig. 4, zino-higgsino mixtures and pure higgsinos are cosmologically relevant above  $\sim 20$  GeV, while binos and photinos are cosmologically relevant above  $\sim 2$  GeV (without grand unification constraints).

### CRESST Set-Up

located in Hall B now moved to Hall A



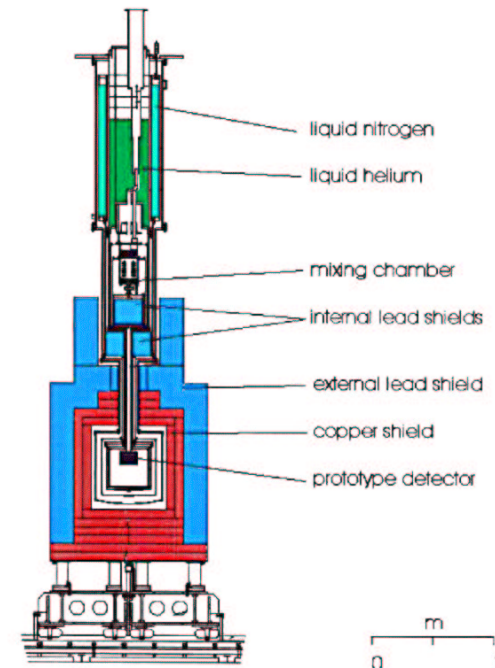
- Cryostat on vibration dampers
- Cryostat placed in a Faraday cage
- Cold-box in clean room (measured class 100)
- Service area easily accessible

### CRESST Set-Up

Specially designed low-background cryostat

Dilution refrigerator

low background cold-box



Only specially selected low background materials

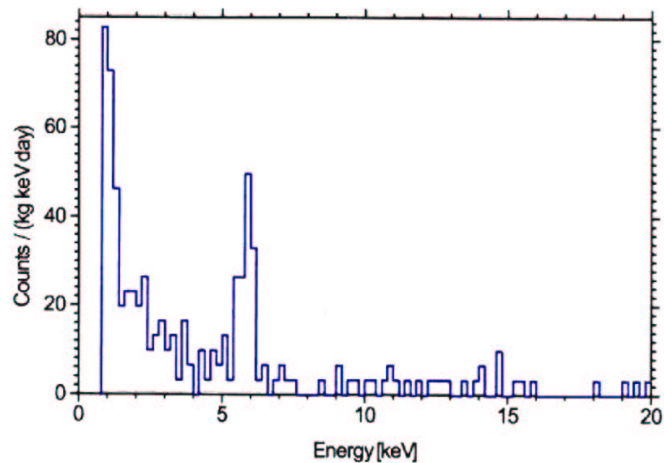
with minimised exposure time to cosmic activation

cold box large enough to house large detector mass (100kg)

## 1,5 kg d Measurement

4\*4\*4 cm<sup>3</sup> sapphire detector (262g) @ 12 mK

threshold 580 eV



Background @15 keV about 1c /kg keV d

Fitted line position 5.9 keV

## WIMP Scattering Cross Sections

The neutralino is the theoretically favoured candidate.

Depending on its composition, neutralinos can have spin dependent and/or spin independent interactions

$$\sigma_{sd} \propto \lambda^2 J(J+1) \quad \text{spin dependent}$$

$$\sigma_{sid} \propto A^2 \quad \text{spin independent}$$

CRESST I optimised for light WIMPs with spin dependent interaction

CRESST II optimised for medium and high mass WIMPs with spin independent interaction



For calculating the energy spectrum of nuclear recoils from elastic collisions between WIMPs and the nuclei of the detector we use formulas from the extensive reviews [8, 9] for a truncated Maxwell velocity distribution in an isothermal WIMP halo model. The parameters which have been used are summarized in table 1. For the spin dependent interaction channel only the  $^{27}\text{Al}$  nuclei with a spin of 5/2 and 100% natural isotopic abundance contribute, while for spin independent interaction Al and O nuclei both contribute with a rate proportional to  $A^2$ .

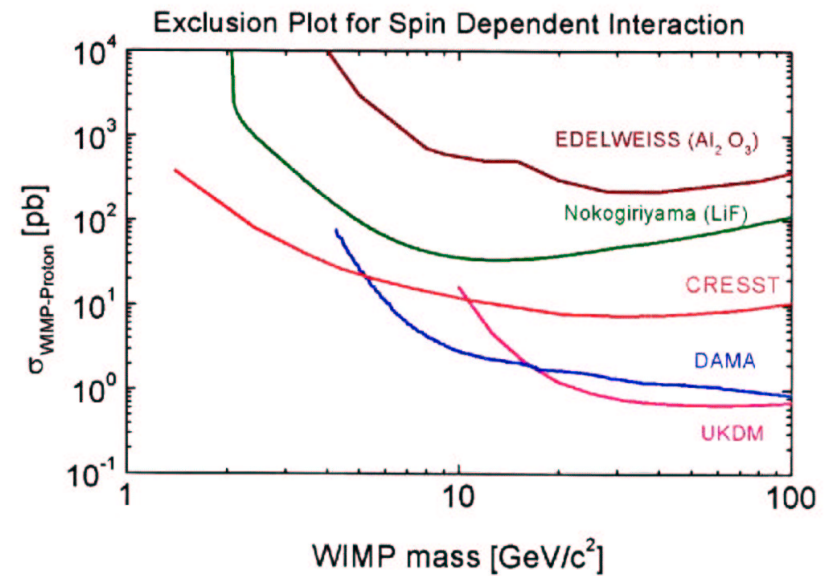
Table 1: List of parameters used for calculating WIMP spectra

Parameter name	value
WIMP velocity distribution	270 km/s
Escape velocity	650 km/s
Earth relative velocity	230 km/s
WIMP local halo density	0.3 $\text{GeV}/\text{cm}^3$

The total WIMP-nucleus scattering cross section  $\sigma(q)$  at finite momentum transfers  $q$  is parameterized as  $\sigma(q) = \sigma_0 F^2(q)$ , where  $\sigma_0$  is the cross section at zero momentum transfer and  $F(q)$  is the form factor which accounts for the loss of coherence at larger momentum transfers. The Helm form factor [10] with the modifications proposed in [8] has been selected for both interaction channels. For small nuclei like  $^{27}\text{Al}$  the momentum transfer is small for all WIMP masses, and details of the form factor have negligible effect on the resulting exclusion plot. Therefore the selected form factor is adequate for both interaction channels. The energy resolution at the 5.9 keV peak in Fig. 10. is  $\delta E = (572 \pm 90)$  eV (FWHM), whereas the resolution of the Fe  $K_{\alpha}$  peak at 6.4 keV from the internal calibration source is  $(200 \pm 50)$  eV in agreement with the energy resolution of the heater pulses. At the 122 keV peak of the calibration source the resolution degrades to about 5 keV. To account for the finite energy resolution of the detector the recoil spectrum was convolved with a Gaussian with an energy dependent full width at half maximum of  $\delta E = \sqrt{a^2 + b^2 E^2}$ . With  $a=0.52$  keV and  $b=4.1$ , this gives  $\delta E = 0.57$  keV and  $\delta E = 5$  keV at  $E=5.9$  keV and  $E=122$  keV, respectively. We further assumed a quenching factor of 1, i.e. 100% of the nuclear recoil energy is detected in the phonon readout channel. An experimental proof of this plausible assumption does not exist up to now for our sapphire detectors. However, quenching factors close to 1 have been measured with other cryogenic detectors [12].

The analysis procedure which has been used to obtain the exclusion curves is Fig. 12 and Fig. 13 works as follows: After calculating the shape of the energy spectrum for a given WIMP mass,  $\sigma_0$  which is the scale factor for the intensity of the WIMP expectation, is determined by a maximum-likelihood comparison of the calculated WIMP spectrum with the measured energy spectrum. The analysis is aiming to find the amount of WIMP events that just too large to be hidden under the measured spectrum. Some energy intervals (typically close to the threshold) are more effective than others for constraining the existence of a WIMP signal in the data. Therefore, it is reasonable to select these energy intervals and use them to give the most stringent exclusion limits on a WIMP signal that can be obtained from the data.

## CRESST I Limits Spin Dependent interaction



Best limits for low WIMP masses

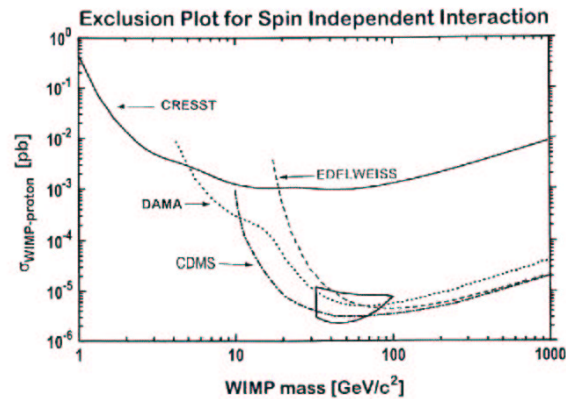


Figure 12: Equivalent WIMP-nucleon cross section limits (90 % CL) for spin-independent interaction as a function of the WIMP mass for 1.51 kg days exposure of a 262g sapphire detector. For comparison DAMA NaI limits with pulse shape discrimination [17], CDMS limits with statistical subtraction of the neutron background [19], limits from the UK dark matter search [18] and from the EDELWEISS WIMP search with a heat and ionization Ge Detector [20] are also shown together with the allowed region at  $3\sigma$  CL for a WIMP r.m.s. velocity of 270 km/s from the DAMA annual modulation data [25].

the likelihoods from the fits of the synthetic data sets. For the curve shown in Fig. 10, 49.1% of the synthetic likelihood values are larger, indicating a perfect choice of the fit function.

The results of these methods are compared in Fig. 11. At low WIMP masses the optimal bin method yields weaker limits. This is connected with the restriction to a 1.2 keV minimal width of the sliding bin which is quite large for very low WIMP masses for which the optimal bin starts at threshold. For WIMP masses above 10 GeV on the other hand the optimal bin is searched in relatively wide region with low statistics which results in a large selection bias. For a WIMP mass from 30 GeV to 1000 GeV for example the region from 22.7 keV to 26.3 keV with no counts inside is selected as the optimal bin. To avoid this bias we have chosen the MC method. The small difference between MC and fitting method still needs further investigation and therefore we consider the results presented here still as preliminary.

In order to compare our results to those of other experiments, we have to normalize the obtained WIMP-nucleus cross sections (for spin-dependent, axial, and spin-independent, scalar, interactions) to WIMP-nucleon cross sections. Following [8, 9], the normalization for the scalar interaction channel is straight forward and yields the results shown in Fig. 12. The scalar channel is not very favourable for a target with light nuclei like sapphire, containing aluminium and oxygen, due to the crucial  $A^2$  coherence factor, especially for higher WIMP masses. That will change with the CRESST-II detectors as explained in the next section.

## CRESST II

### Goals:

- Search for WIMP Dark Matter  $m_w > 35 \text{ GeV}$
- High sensitivity
- 10kg total mass

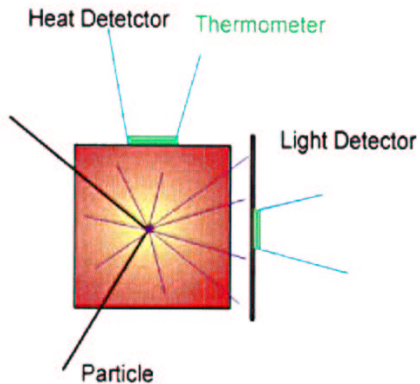
### Detector Concept:

- Cryogenic Detector
- Background discrimination due to simultaneous detection of phonons and scintillation light
- Absorber material with heavy nuclei  $\sigma_w \sim A^2$



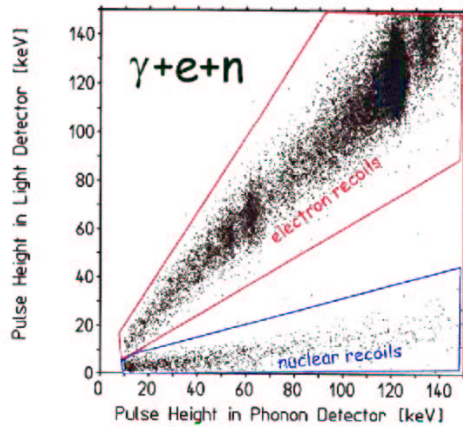
## Detector Concept

Background discrimination by simultaneous detection of phonons and light



Works with many absorber materials  
 $\text{CaWO}_4, \text{PbWO}_4, \text{BaF}, \text{BGO}$   
 (other tungstates and molybdates)

light detector is a cryo-detector of CRESST type



High rejection:

99.7%  $E > 15 \text{ keV}$

99.9%  $E > 20 \text{ keV}$

Appl. Phys.Lett.  
 75(9),1335(1999)

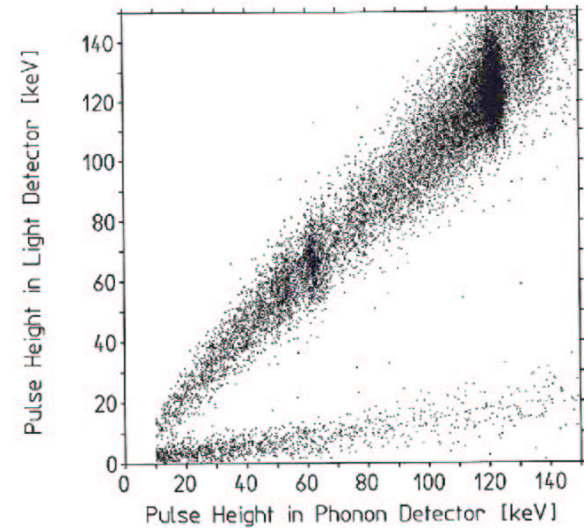


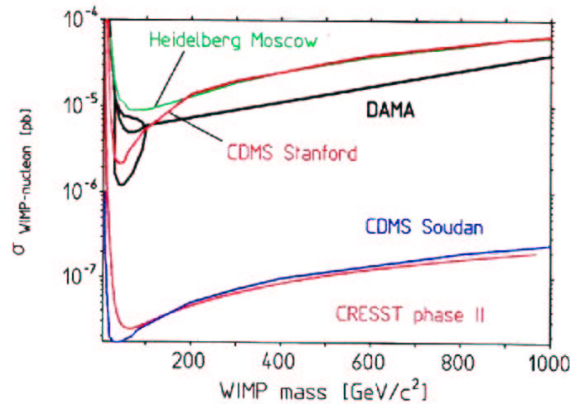
Figure 14: Pulse height in the light detector versus pulse height in the 6g  $\text{CaWO}_4$  phonon detector, measured while the detector was irradiated with photons, electrons, and neutrons. The lower band is caused by neutron-induced nuclear recoils, the diagonal band by recoils from photons and electrons.

## Planned Experiment and Expected Performance

Detector mass:  
10 kg based on 33 modules of 300g

Detector Material:  $\text{CaWO}_4$   
Rejection: 99.7 for  $E > 15 \text{ keV}$

### Fits into present set-up



Exposure:  
30 kg years

$E_{th} = 15 \text{ keV}$

Background:  
1c/kg keV d

Rejection:  
99.7 %

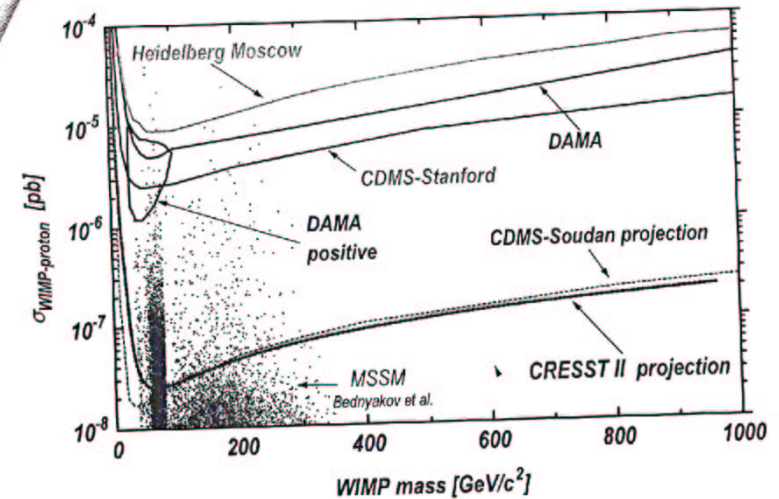


Figure 15: WIMP-nucleon cross section limits (90% CL) for spin-independent interactions as a function of the WIMP mass, expected for a 10 kg  $\text{CaWO}_4$  detector with a background rejection of 99.7% above a threshold of 15 keV detector and 3 years of measurement time in the CRESST set-up in Gran Sasso. For comparison the measured limit from the Heidelberg-Moscow  $^{76}\text{Ge}$  experiment [23], the DAMA NaI limits [24] and contour for positive evidence [25], the CDMS Stanford limit [19] and the expectation for CDMS Soudan [26] are also shown. The scatter plot shows the expectations for WIMP-neutralinos calculated in the MSSM framework with non-universal scalar mass unification [27].

to 66. Additionally we plan to install an external muon veto and a passive neutron shield. These upgrades are being implemented during 2001 as part of our move from Hall B to Hall A of Gran Sasso.

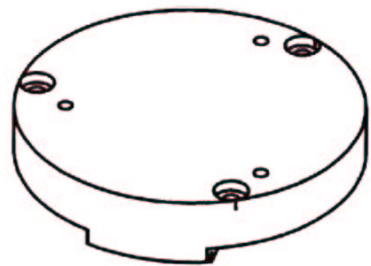
### 3.2 Expected dark matter sensitivity

The presence of the heavy tungsten nuclei make the new detectors particularly sensitive to a spin-independent interaction of WIMPs, for which the cross section profits from a large coherence factor of the order  $A^2$ , where  $A$  is the number of nucleons. Combined with the strong background rejection, this gives good sensitivity down to low WIMP cross sections. Fig. 15 shows the expected sensitivity of Phase II, based on a background rate of 1 count/(kg keV day), an intrinsic background rejection of 99.7% above a recoil threshold of 15 keV, and an exposure of 30 kg years. For comparison the measured limits from the

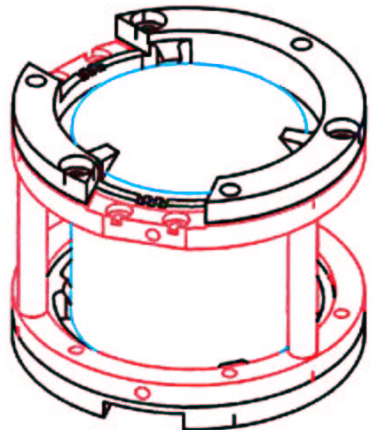


### Detector Element

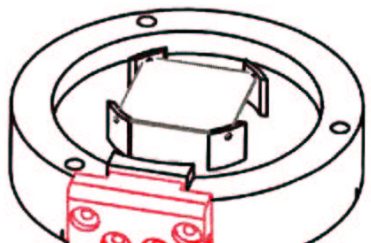
CaWO<sub>4</sub> crystal, mass 300g



Diffusive reflector endcaps

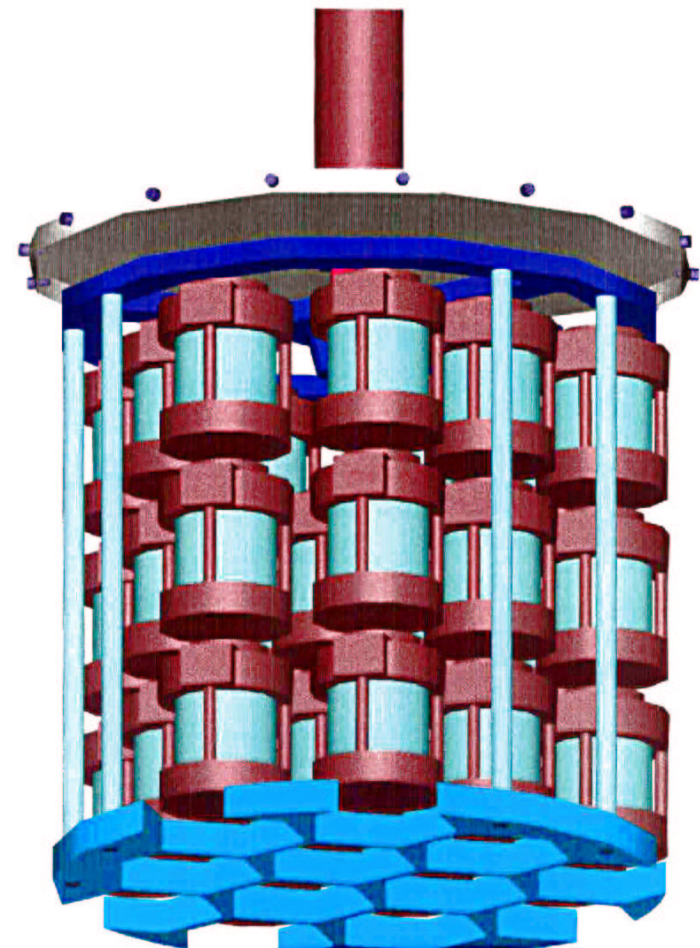


300g CaWO<sub>4</sub> in specular reflector



Diffusive reflector endcap + light detector

### Detector Arrangement





## Potential of CRESST II

- Good background rejection ( electrons and photons)
- relatively high detector mass
- Can use choice of absorber materials with different nuclear composition (important for verification of a positive signal and determination of the nature of WIMPs)  
CaWO<sub>4</sub>, BaF, PbWO<sub>4</sub>, BGO....
- Set-up already exists (upgrade of read-out channels and neutron shield needed)

## Status and Schedule of CRESST II

- Approved and financed
- First Prototypes ready
- 2002 prototype test
- 2003 read out + neutron shield upgrade  
start first measurements